

Ligand field and anions-driven structures and magnetic properties of dysprosium complexes

Shao-Min Xu,^a Zhong-Wu An,^a Wei Zhang,^a Yi-Quan Zhang^{*b} and Min-Xia Yao^{*a}

^a College of Chemistry & Molecular Engineering, Nanjing Tech University, Nanjing, 211816, P. R. China.

^b Jiangsu Key Lab for NSLSCS, School of Physical Science and Technology, Nanjing Normal University, Nanjing 210023, China.

Table S1 Selected bond lengths (Å) and angles (°) for **1**.

Dy(1)-O(2)	2.204(4)	Dy(1)-O(1)	2.261(4)
Dy(1)-O(3)	2.415(4)	Dy(1)-N(3)	2.479(4)
Dy(1)-N(5)	2.527(5)	Dy(1)-N(2)	2.550(5)
Dy(1)-N(1)	2.553(5)	Dy(1)-N(4)	2.620(5)
O(2)-Dy(1)-O(1)	149.74(2)	O(2)-Dy(1)-O(3)	131.55(2)
O(1)-Dy(1)-O(3)	78.40(1)	O(2)-Dy(1)-N(3)	76.28(2)
O(1)-Dy(1)-N(3)	78.18(1)	O(3)-Dy(1)-N(3)	145.48(2)
O(2)-Dy(1)-N(5)	92.16(2)	O(1)-Dy(1)-N(5)	92.88(2)
O(3)-Dy(1)-N(5)	74.34(2)	N(3)-Dy(1)-N(5)	131.80(2)
O(2)-Dy(1)-N(2)	103.99(2)	O(1)-Dy(1)-N(2)	80.09(1)
O(3)-Dy(1)-N(2)	84.69(1)	N(3)-Dy(1)-N(2)	66.55(2)
N(5)-Dy(1)-N(2)	158.86(2)	O(2)-Dy(1)-N(1)	70.10(2)
O(1)-Dy(1)-N(1)	135.56(2)	O(3)-Dy(1)-N(1)	70.48(2)
N(3)-Dy(1)-N(1)	111.40(2)	N(5)-Dy(1)-N(1)	107.79(2)
N(2)-Dy(1)-N(1)	66.42(2)	O(2)-Dy(1)-N(4)	74.10(2)
O(1)-Dy(1)-N(4)	81.06(1)	O(3)-Dy(1)-N(4)	133.20(1)
N(3)-Dy(1)-N(4)	66.63(2)	N(5)-Dy(1)-N(4)	65.21(2)
N(2)-Dy(1)-N(4)	132.08(2)	N(1)-Dy(1)-N(4)	143.26(2)

Table S2 Selected bond lengths (Å) and angles (°) for **2**.

Dy(1)-O(1)	2.188(2)	Dy(1)-O(2)	2.224(1)
Dy(1)-O(4)	2.498(1)	Dy(1)-N(3)	2.550 (2)
Dy(1)-O(3)	2.583(1)	Dy(1)-N(5)	2.646(2)
Dy(1)-N(2)	2.652(2)	Dy(1)-N(4)	2.679(2)

* To whom correspondence should be addressed. Email: yaomx@njtech.edu.cn; zhangyiquan@njnu.edu.cn Fax: +86-25-58139528.

Dy(1)-N(1)	2.712(2)	O(1)-Dy(1)-O(2)	148.62(5)
O(1)-Dy(1)-O(4)	127.55(5)	O(2)-Dy(1)-O(4)	82.10(5)
O(1)-Dy(1)-N(3)	80.82(6)	O(2)-Dy(1)-N(3)	80.00(6)
O(4)-Dy(1)-N(3)	140.24(5)	O(1)-Dy(1)-O(3)	79.93(5)
O(2)-Dy(1)-O(3)	123.59(5)	O(4)-Dy(1)-O(3)	49.92(5)
N(3)-Dy(1)-O(3)	155.68(5)	O(1)-Dy(1)-N(5)	75.09(6)
O(2)-Dy(1)-N(5)	131.59(6)	O(4)-Dy(1)-N(5)	70.42(5)
N(3)-Dy(1)-N(5)	96.23(6)	O(3)-Dy(1)-N(5)	64.45(6)
O(1)-Dy(1)-N(2)	74.48(5)	O(2)-Dy(1)-N(2)	75.14(5)
O(4)-Dy(1)-N(2)	140.73(6)	N(3)-Dy(1)-N(2)	66.28(5)
O(3)-Dy(1)-N(2)	121.74(5)	N(5)-Dy(1)-N(2)	146.90(6)
O(1)-Dy(1)-N(4)	115.90(6)	O(2)-Dy(1)-N(4)	75.89(5)
O(4)-Dy(1)-N(4)	78.96(5)	N(3)-Dy(1)-N(4)	62.36(5)
O(3)-Dy(1)-N(4)	114.09(5)	N(5)-Dy(1)-N(4)	60.53(5)
N(2)-Dy(1)-N(4)	124.16(5)	O(1)-Dy(1)-N(1)	96.52(6)
O(2)-Dy(1)-N(1)	76.60(5)	O(4)-Dy(1)-N(1)	80.56(5)
N(3)-Dy(1)-N(1)	128.29(5)	O(3)-Dy(1)-N(1)	68.85(5)
N(5)-Dy(1)-N(1)	133.30(6)	N(2)-Dy(1)-N(1)	63.40(5)
N(4)-Dy(1)-N(1)	147.57(5)		

Table S3 Selected bond lengths (\AA) and angles ($^\circ$) for **3**.

Dy(1)-O(2)	2.286 (2)	Dy(1)-O(1)	2.313(2)
Dy(1)-O(3)	2.328(2)	Dy(1)-O(4)	2.342(2)
Dy(1)-N(3)	2.478(2)	Dy(1)-N(1)	2.492(2)
Dy(1)-N(4)	2.578(2)	Dy(1)-N(2)	2.608(2)
Dy(2)-O(8)	2.323(2)	Dy(2)-O(6)	2.339(2)
Dy(2)-O(9)	2.345(2)	Dy(2)-O(7)	2.368(2)
Dy(2)-O(5)	2.370(2)	Dy(2)-O(10)	2.372(2)
Dy(2)-O(1)	2.407(2)	Dy(2)-O(2)	2.430(2)
O(2)-Dy(1)-O(1)	68.63(6)	O(2)-Dy(1)-O(3)	148.87(6)
O(1)-Dy(1)-O(3)	142.29(6)	O(2)-Dy(1)-O(4)	79.40(6)
O(1)-Dy(1)-O(4)	147.11(6)	O(3)-Dy(1)-O(4)	70.30(6)
O(2)-Dy(1)-N(3)	130.19(6)	O(1)-Dy(1)-N(3)	78.82(6)
O(3)-Dy(1)-N(3)	69.80(6)	O(4)-Dy(1)-N(3)	130.47(6)
O(2)-Dy(1)-N(1)	88.35(7)	O(1)-Dy(1)-N(1)	94.21(7)
O(3)-Dy(1)-N(1)	91.56(7)	O(4)-Dy(1)-N(1)	76.89(7)
N(3)-Dy(1)-N(1)	131.82(7)	O(2)-Dy(1)-N(4)	77.32(6)
O(1)-Dy(1)-N(4)	92.74(6)	O(3)-Dy(1)-N(4)	94.00(6)

O(4)-Dy(1)-N(4)	87.46(7)	N(3)-Dy(1)-N(4)	67.44(7)
N(1)-Dy(1)-N(4)	160.54(7)	O(2)-Dy(1)-N(2)	135.01(6)
O(1)-Dy(1)-N(2)	76.97(6)	O(3)-Dy(1)-N(2)	71.66(6)
O(4)-Dy(1)-N(2)	124.80(6)	N(3)-Dy(1)-N(2)	66.26(7)
N(1)-Dy(1)-N(2)	65.73(7)	N(4)-Dy(1)-N(2)	133.67(7)
O(8)-Dy(2)-O(6)	73.97(6)	O(8)-Dy(2)-O(9)	85.02(6)
O(6)-Dy(2)-O(9)	142.15(6)	O(8)-Dy(2)-O(7)	71.46(6)
O(6)-Dy(2)-O(7)	125.80(6)	O(9)-Dy(2)-O(7)	73.49(6)
O(8)-Dy(2)-O(5)	101.56(6)	O(6)-Dy(2)-O(5)	70.31(6)
O(9)-Dy(2)-O(5)	146.17(6)	O(7)-Dy(2)-O(5)	77.28(6)
O(8)-Dy(2)-O(10)	73.55(6)	O(6)-Dy(2)-O(10)	73.97(6)
O(9)-Dy(2)-O(10)	69.98(6)	O(7)-Dy(2)-O(10)	130.78(6)
O(5)-Dy(2)-O(10)	143.80(6)	O(8)-Dy(2)-O(1)	149.62(6)
O(6)-Dy(2)-O(1)	133.75(6)	O(9)-Dy(2)-O(1)	76.80(6)
O(7)-Dy(2)-O(1)	80.05(5)	O(5)-Dy(2)-O(1)	81.78(6)
O(10)-Dy(2)-O(1)	120.83(6)	O(8)-Dy(2)-O(2)	144.26(6)
O(6)-Dy(2)-O(2)	79.17(6)	O(9)-Dy(2)-O(2)	103.01(6)
O(7)-Dy(2)-O(2)	144.27(6)	O(5)-Dy(2)-O(2)	90.89(6)
O(10)-Dy(2)-O(2)	76.70(6)	O(1)-Dy(2)-O(2)	64.82(5)

Table S4 Continuous Shape Measures (CShMs) of the coordination geometry for Dy (III) ion in compounds **1-3**. Below is the symmetry and description for each polyhedron.

Complex		CU-8	SAPR-8	TDD-8
1		8.953	3.922	2.925
3	Dy1	12.018	3.564	1.131
	Dy2	9.145	1.526	0.705
CU-8	O _h	Cube		
SAPR-8	D _{4d}	Square antiprism		
TDD-8	D _{2d}	Triangular dodecahedron		
Complex		JTCTPR-9	JCSAPR-9	CSAPR-9
2		3.314	3.529	2.836
JTCTPR-9	D _{3h}	Tricapped trigonal prism J51		
JCSAPR-9	C _{4v}	Capped square antiprism J10		
CSAPR-9	C _{4v}	Spherical capped square antiprism		

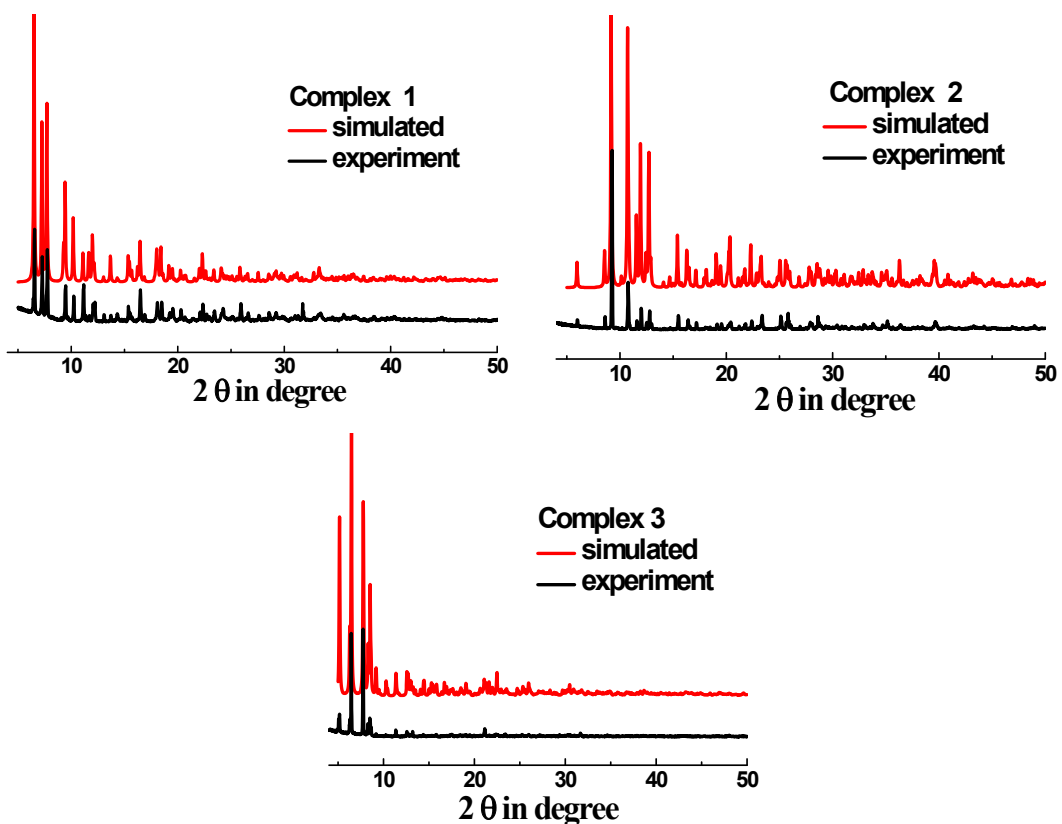


Fig. S1 PXRD patterns for complexes 3

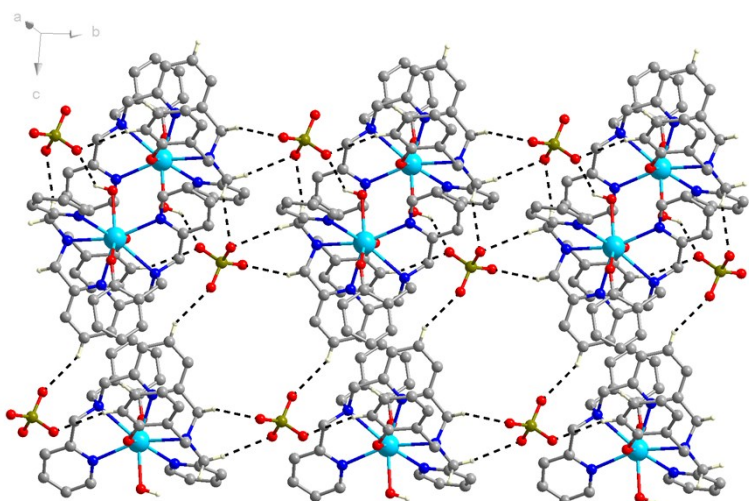


Fig. S2. A view showing 3D structure formed by weak C-H...O and O-H...O hydrogen bonds interactions in **1**.

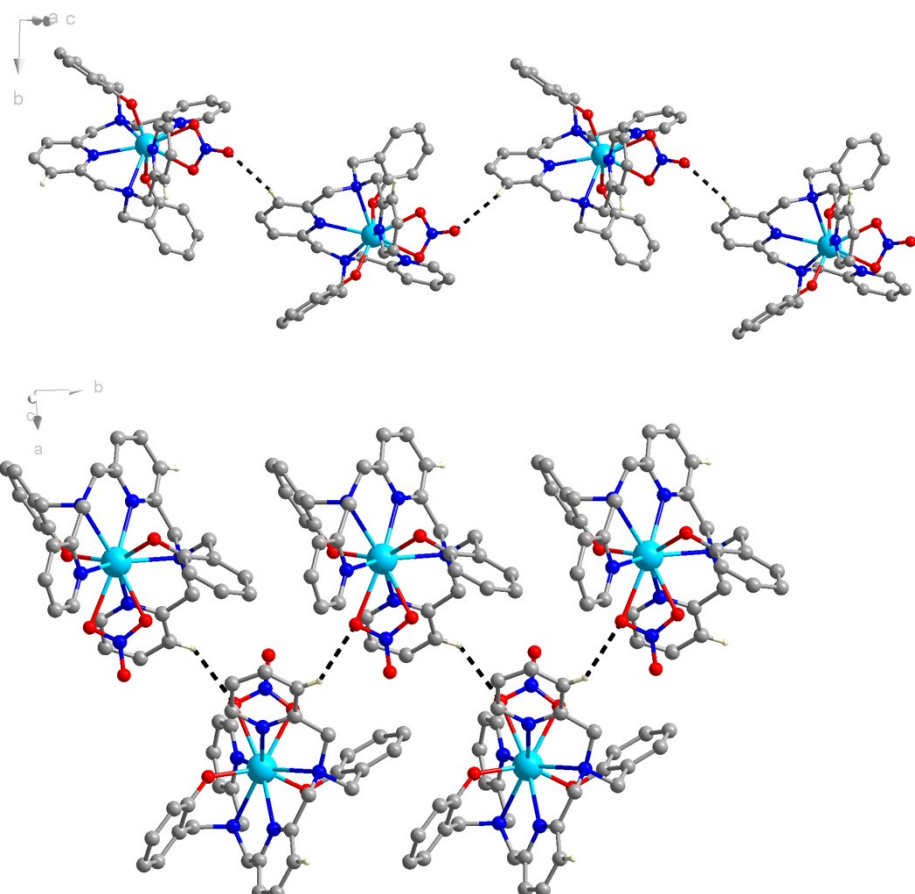


Fig. S3. A view showing 3D structure formed by weak C–H \cdots O hydrogen bonds interactions in **2**.

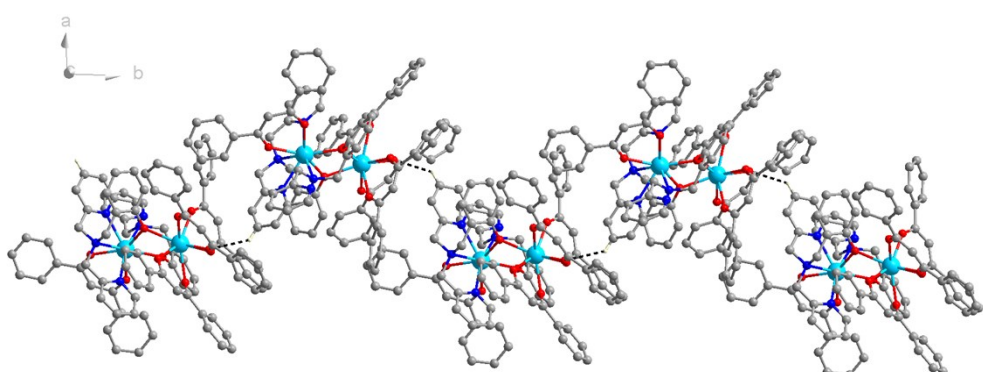


Fig. S4. A view showing 3D structure formed by weak C–H \cdots O, C–H \cdots C and π – π stacking interactions in **3**.

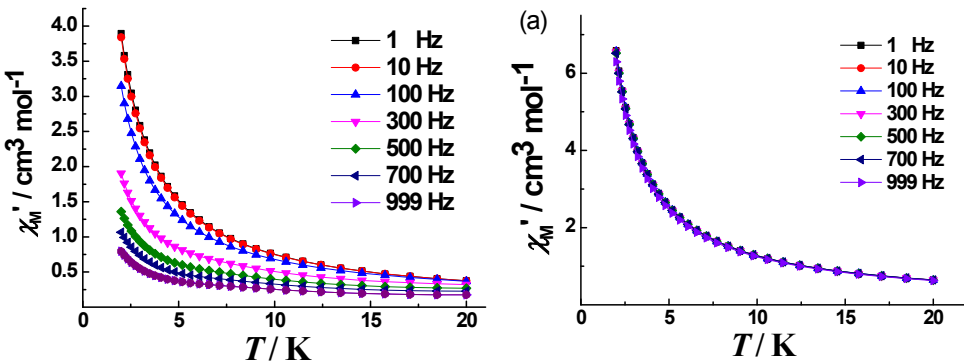


Fig.S5 Temperature dependence of the in-phase (χ') of the ac susceptibility for **2** (left) and **3** (right) under a zero applied dc.

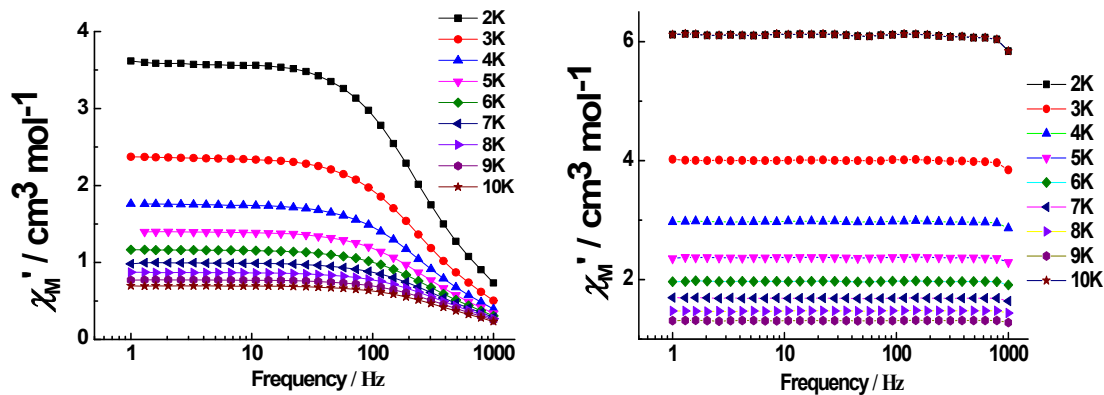


Fig.S6 Frequency dependence of the in-phase (χ') ac susceptibility signals for **2** (left) and **3** (right) under a zero-dc field.

Computational details

Mononuclear complexes **1** and **2** have one type of molecular structure, but binuclear complex **3** has two types of magnetic center Dy^{III} ions indicated as **3_Dy1** and **3_Dy2**. Complete-active-space self-consistent field (CASSCF) calculations on complexes **1–3** (see Figure S7 for the calculated complete structures of complexes **1–3**) on the basis of single-crystal X-ray determined geometry have been carried out with MOLCAS 8.4^{S1} program package. Each individual Dy^{III} fragment in **3** was calculated keeping the experimentally determined structure of the corresponding compound while the neighboring Dy^{III} ion was replaced by diamagnetic Lu^{III}.

The basis sets for all atoms are atomic natural orbitals from the MOLCAS ANO-RCC library: ANO-RCC-VTZP for Dy^{III}; VTZ for close N and O; VDZ for distant atoms. The calculations employed the second order Douglas-Kroll-Hess Hamiltonian, where scalar relativistic contractions were taken into account in the basis set and the spin-orbit couplings were handled separately in the

restricted active space state interaction (RASSI-SO) procedure. For individual Dy^{III} fragment, active electrons in 7 active spaces include all *f* electrons (CAS(9 in 7)) in the CASSCF calculation. To exclude all the doubts, we calculated all the roots in the active space. We have mixed the maximum number of spin-free state which was possible with our hardware (all from 21 sextets, 128 from 224 quadruplets, 130 from 490 doublets). SINGLE_ANISO^{S2} program was used to obtain the energy levels, *g* tensors, *m_J* values, magnetic axes, *et al.* based on the above CASSCF/RASSI-SO calculations.

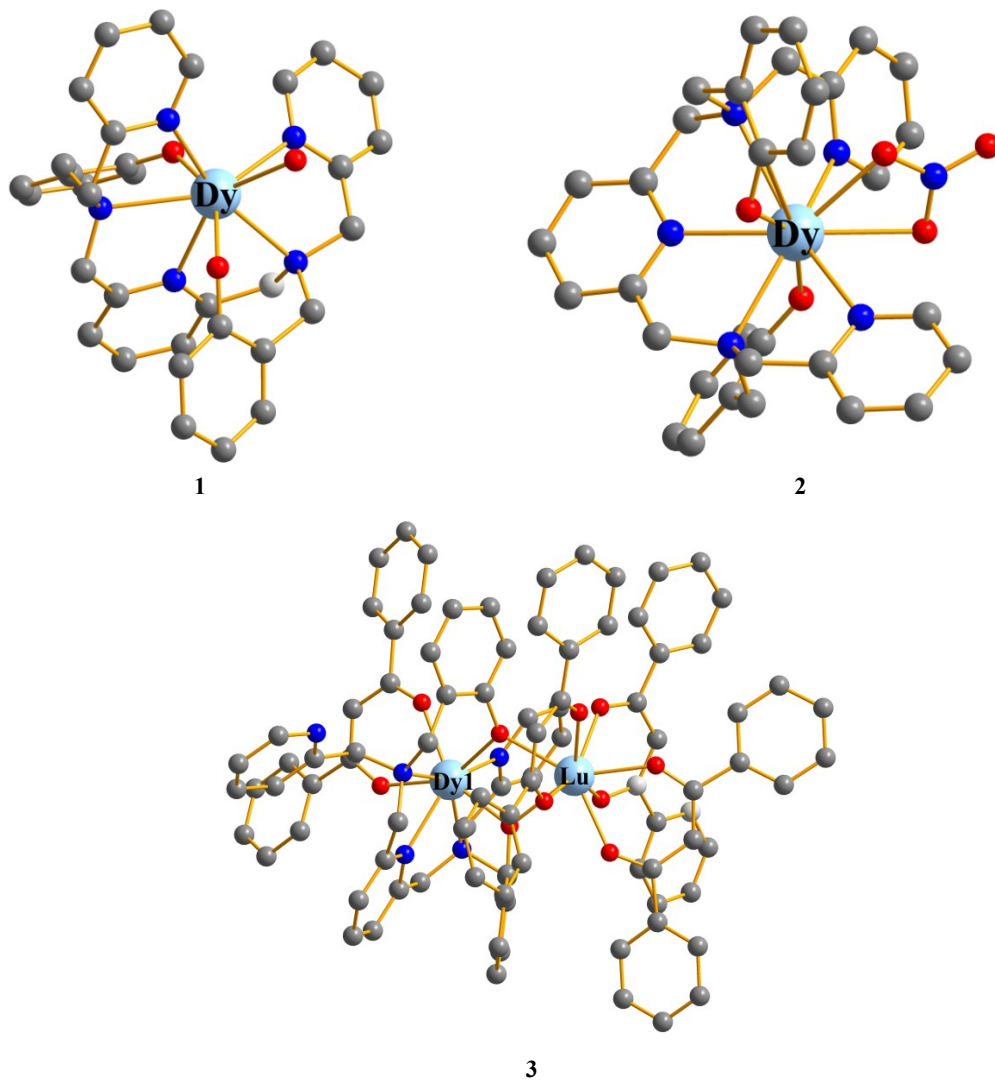


Fig. S7. Calculated complete structures of **1–3**; H atoms are omitted.

Table S5. Calculated energy levels (cm^{-1}), *g* (g_x , g_y , g_z) tensors and predominant m_J values of the lowest eight Kramers doublets (KDs) of individual Dy^{III} fragments for **1–3** using CASSCF/RASSI-SO with MOLCAS 8.4.

KDs	1			2		
	E/cm^{-1}	<i>g</i>	m_J	E/cm^{-1}	<i>g</i>	m_J
1	0.0 0.005	0.004 0.005	$\pm 15/2$	0.0 0.002	0.002 0.002	$\pm 15/2$

		19.811		19.851		
		0.100		0.044		
2	284.4	0.120	$\pm 13/2$	277.7	0.053	$\pm 13/2$
		16.950			16.985	
		0.512			0.101	
3	498.1	0.635	$\pm 11/2$	512.2	0.171	$\pm 11/2$
		13.628			13.922	
		5.189			4.221	
4	617.5	5.379	$\pm 9/2$	662.1	6.090	$\pm 9/2$
		7.910			8.985	
		1.291			1.329	
5	666.7	3.396	$\pm 1/2$	740.1	3.656	$\pm 5/2$
		13.589			12.828	
		0.085			1.744	
6	697.5	0.841	$\pm 3/2$	796.4	4.509	$\pm 3/2$
		15.334			9.312	
		0.274			1.063	
7	785.0	1.881	$\pm 7/2$	813.3	6.764	$\pm 1/2$
		17.226			13.023	
		0.023			0.105	
8	809.1	2.161	$\pm 5/2$	904.0	0.336	$\pm 7/2$
		17.423			18.895	

KDs	3_Dy1			3_Dy2		
	<i>E/cm</i> ⁻¹	<i>g</i>	<i>m_J</i>	<i>E/cm</i> ⁻¹	<i>g</i>	<i>m_J</i>
		0.110			0.028	
1	0.0	0.252	$\pm 15/2$	0.0	0.098	$\pm 15/2$
		19.198			19.272	
		1.169			0.209	
2	132.2	1.842	$\pm 13/2$	60.2	0.268	$\pm 1/2$
		15.660			18.598	
		4.174			0.741	
3	237.4	4.439	$\pm 11/2$	104.2	1.191	$\pm 11/2$
		10.113			13.690	
		2.270			3.726	
4	336.9	3.911	$\pm 7/2$	149.6	5.705	$\pm 5/2$
		9.747			8.415	
		0.057			1.721	
5	441.6	1.919	$\pm 5/2$	175.9	4.776	$\pm 7/2$
		12.266			14.364	
		0.810			0.324	
6	498.4	1.203	$\pm 3/2$	192.9	1.208	$\pm 9/2$
		15.396			18.247	
7	536.1	0.207	$\pm 1/2$	215.3	0.034	$\pm 3/2$

		0.309		0.307	
		17.342		19.355	
		0.033		0.000	
8	653.5	0.054	$\pm 9/2$	382.2	0.003 $\pm 13/2$
		19.466		19.731	

Table S6. Wave functions with definite projection of the total moment $|m_J\rangle$ for the lowest two KDs of individual Dy^{III} fragments for **1–3**, respectively, using CASSCF/RASSI-SO with MOLCAS 8.4.

	E/cm^{-1}	wave functions
1	0.0	98.82% $\pm 15/2\rangle$
	284.4	94.90% $\pm 13/2\rangle$
2	0.0	99.81% $\pm 15/2\rangle$
	277.7	98.82% $\pm 13/2\rangle$
3_Dy1	0.0	88.87% $\pm 15/2\rangle + 9.71\% \pm 11/2\rangle$
	132.2	45.93% $\pm 13/2\rangle + 28.18\% \pm 9/2\rangle + 8.23\% \pm 7/2\rangle + 6.05\% \pm 5/2\rangle$
3_Dy2	0.0	89.54% $\pm 15/2\rangle + 9.09\% \pm 11/2\rangle$
	60.2	41.46% $\pm 1/2\rangle + 29.54\% \pm 3/2\rangle + 14.53\% \pm 5/2\rangle$

To fit the exchange interaction in **3**, we took two steps to obtain them. Firstly, we calculated individual Dy^{III} fragments using CASSCF/RASSI-SO to obtain the corresponding magnetic properties. Then, the exchange interaction between the magnetic centers is considered within the Lines model,^{S3} while the account of the dipole-dipole magnetic coupling is treated exactly. The Lines model is effective and has been successfully used widely in the research field of *d* and *f*-elements single-molecule magnets.^{S4}

The Ising exchange Hamiltonians for **3** is:

$$\hat{H}_{\text{exch}} = -J\hat{S}_{\text{Dy1}}\hat{S}_{\text{Dy2}} \quad (1)$$

The $J = 25\cos\varphi J_{\text{exch}}$, where φ is the angle between the anisotropy axes on sites Dy1 and Dy2, and J_{exch} is the Lines exchange coupling parameter. The $S_{\text{Dy}} = 1/2$ is the ground pseudospin on the Dy^{III} sites. The dipolar magnetic coupling can be calculated exactly, while the exchange coupling constant was fitted through comparison of the computed and measured magnetic susceptibility using the POLY_ANISO program.^{S2}

Table S7. Exchange energies E (cm^{-1}), the energy difference between each exchange doublets Δ_t (cm^{-1}) and the main values of the g_z for the lowest two exchange doublets of **3**.

	E	Δ_t	g_z
1	0.0	1.2×10^{-3}	22.704
2	2.0	1.0×10^{-3}	30.909

References:

- S1 F. Aquilante, J. Autschbach, R. K. Carlson, L. F. Chibotaru, M. G. Delcey, L. De Vico, I. Fdez. Galván, N. Ferré, L. M. Frutos, L. Gagliardi, M. Garavelli, A. Giussani, C. E. Hoyer, G. Li Manni, H. Lischka, D. Ma, P. Å. Malmqvist, T. Müller, A. Nenov, M. Olivucci, T. B. Pedersen, D. Peng, F. Plasser, B. Pritchard, M. Reiher, I. Rivalta, I. Schapiro, J. Segarra - Martí, M. Stenrup, D. G. Truhlar, L. Ungur, A. Valentini, S. Vancoillie, V. Veryazov, V. P. Vysotskiy, O. Weingart, F. Zapata, R. Lindh, MOLCAS 8: New Capabilities for Multiconfigurational Quantum Chemical Calculations across the Periodic Table, *J. Comput. Chem.*, **2016**, *37*, 506–541.
- S2 (a) Chibotaru, L. F.; Ungur, L.; Soncini, A. *Angew. Chem. Int. Ed.*, **2008**, *47*, 4126–4129. (b) Ungur, L.; Van den Heuvel, W.; Chibotaru, L. F. *New J. Chem.*, **2009**, *33*, 1224–1230. (c) Chibotaru, L. F.; Ungur, L.; Aronica, C.; Elmoll, H.; Pilet, G.; Luneau, D. *J. Am. Chem. Soc.*, **2008**, *130*, 12445–12455.
- S3 Lines, M. E. *J. Chem. Phys.* **1971**, *55*, 2977–2984.
- S4 (a) Mondal, K. C.; Sundt, A.; Lan, Y. H.; Kostakis, G. E.; Waldmann, O.; Ungur, L.; Chibotaru, L. F.; Anson, C. E.; Powell, A. K. *Angew. Chem. Int. Ed.* **2012**, *51*, 7550–7554. (b) Langley, S. K.; Wielechowski, D. P.; Vieru, V.; Chilton, N. F.; Moubaraki, B.; Abrahams, B. F.; Chibotaru, L. F.; Murray, K. S. *Angew. Chem. Int. Ed.* **2013**, *52*, 12014–12019.